Anti-shock pneumohydraulic damper

U. Jonkobilov[1], and *S.* Jonkobilov[2]

[1]Higher military aviation educational institution of the Republic of Uzbekistan, Karshi, Uzbekistan
[2]Karshi engineering economic institute, Karshi, Uzbekistan

Abstract. The article is devoted to the analytical calculation of the main parameters and dimensions of a pneumohydraulic hydraulic shock damper with a decrease in pressure installed at the beginning of a pressure pipeline to reduce the emergency consequences of the intensity of shock waves, taking into account the polytropic process of air in the damper. Based on the results of analytical studies of the wave equations of non-stationary pressure movements for the proposed hydraulic shock damper, dependences were obtained for calculating the maximum and minimum impact heads in the first period of pressure fluctuations, considering the polytropic index.
To substantiate the reliability of the proposed dependencies and the economic dimensions of the damper design, comparative calculations of analytical studies with experimental data and data from other authors were performed. Comparative calculations prove the reliability of the proposed dependences obtained by the analytical method of solutions to the known equations of motion of hydromechanics, continuity, and state of the air in the damper.

1 Introduction

Currently, to dampen the force of hydraulic shock that occurs in a long pressure pipeline, pneumohydraulic dampers are widely used [1-7]. Similar anti-shock devices (dampers) can protect water supply pipelines from water hammers. When installing a damper at the beginning of pressure pipelines of pumping stations, their dimensions are determined by the conditions for starting and stopping pumps [3, 4, 7, 8, 9]. Dampers are calculated in different ways according to the conditions for stopping the pumps. Still, the most common method is to select the damper volume according to Evangelisti graphs, compiled from approximate integration of differential equations of unsteady fluid motion using the finite difference method [5]. However, these graphs are calculated only for a very small change interval in the main parameters of pressure pipelines of pumping stations during hydraulic shock in the presence of dampers. There is no general solution in Evangelisti's work; therefore, in many cases, this method is not applicable [4-6].

2 Materials and methods

When solving the problem of determining the main parameters and dimensions of hydraulic shock dampers in a pipeline in a general form, in the presence of dampers in the place of perturbation of the flow, the following three equations are used [3, 7, 10, 11].
The differential equation of acting forces obtained as a result of transformations of the known Navier-Stokes dependences and having the form [3, 7, 10]

$$-\frac{\partial \vartheta}{\partial t}+\frac{\beta}{2}\frac{\partial(\vartheta^2)}{\partial x}+\frac{\partial H}{\partial x}g\pm\frac{\tau_{ну}}{\rho R}=0. \qquad (1)$$

Flow continuity equation in a pressure pipeline in the presence of a damper [3,7,10]

$$dV_1 = Qdt. \qquad (2)$$

The equation expressing the law of change in the volume of air in the damper has the following form [3,7,10]

$$V=V_{\Gamma}\left(\frac{H_{o-a}}{H}\right)^{1/n}. \qquad (3)$$

The above equations have the following notation:

ϑ and H are flow velocity and the absolute pressure in the pipeline at the damper installation site at time t; Q is flow rate of the fluid during steady motion; β is coefficient of momentum; x is coordinate along the length of the pipeline; ρ is liquid density; R is hydraulic radius of the pipe; τ_{nu} is shear stress at the pipe wall in unsteady flow; g is acceleration of gravity; V is volume of air in the damper at the moment t; V_1 is increase in the volume of air in the damper; $V_г$ is volume of air in the damper at the absolute geodetic head H_{o-a} (Fig. 1); n is polytropic index [3, 4].

The accuracy of calculating the hydraulic shock damper depends on the reliable value of the polytropic index n [3,4]. In engineering practice, there is a problem with the selection of the numerical value of the polytropic index n, which considers the law of compression and expansion of air in the hydraulic shock damper [3, 4]. So, for example, N.E. Zhukovsky, when calculating a hydraulic shock damper, takes the process as adiabatic and recommends taking n = 1.41 [1]. In works [2, 3], the authors also accept the law of compression-expansion of air in the damper as adiabatic, and other researchers [5,6,7] accept n=1.0, assuming that the process of compression-expansion of air in the damper is isothermal. At the same time, it is stated in [9, 10, 11] that air compression and expansion in the damper proceeds according to the polytropic law. However, the latter provision requires further elaboration. Therefore, the rationale for the correct choice of the numerical value of the polytropic index for calculating the damper during water hammer is very important [4, 12-15] since the reliability of determining the main economic dimensions of the damper, as well as the minimum and maximum pressure in it, depends on this [16-20].

In this paper, the law of change in the air volume in the damper is adopted as a polytropic process, and the value of the polytropic index n=1.2 is experimentally substantiated in [3, 4].

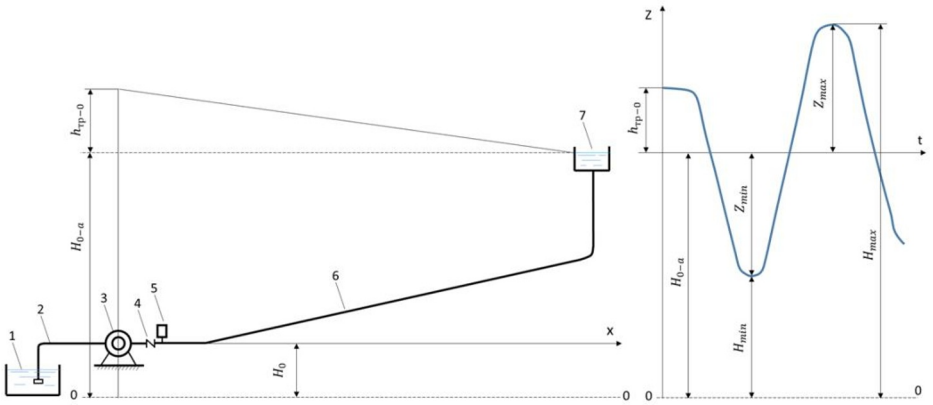

Fig. 1. The change in pressure in the pressure pipeline during steady motion (a) and the change in pressure at the pneumohydraulic damper during hydraulic shock (b): 1 is source of water; 2 is suction pipeline; 3 is pump; 4 is check valve; 5 is damper; 6 is pressure pipeline; 7 is head basin.

In equation (1), as usual [3, 4, 6, 7], the term containing the convective acceleration is neglected due to its smallness. Then for $\tau_{nu}=\lambda_{nu}\rho\vartheta^2/8$ and R=D/4, it turns out

$$-\frac{\partial \vartheta}{\partial t}+\frac{\partial H}{\partial x}g \mp \lambda_{ну}\frac{\vartheta^2}{2D}=0 \qquad (4)$$

Where λ_{nu} is coefficient of hydraulic resistance during hydraulic shock; D is diameter of the pressure pipeline.
In the case of a one-dimensional fluid flow in a pressure pipeline

$$\frac{\partial \vartheta}{\partial t}\approx\frac{d\vartheta}{dt} \qquad (5)$$

The partial derivative $\partial H/\partial x$ is approximately replaced by the increment ratio $\Delta H/\Delta l$, where $\Delta H=H-H_{0\text{-}a}=Z$ is the change in the head during hydraulic shock relative to the geodetic head (see Fig. 1); $\Delta l=l_2-l_1$ is the length of the pressure pipeline under consideration.
Taking into account the above, equation (4) can be written

$$z=\frac{l}{g}\frac{d\vartheta}{dt}\pm\lambda_{ну}\frac{l\vartheta^2}{D2g}=\frac{ld\vartheta}{gdt}\pm h_{\omega} \qquad (6)$$

h_ω - pressure loss along the length of the pressure pipeline during hydraulic shock ($h_\omega=\alpha\vartheta^2$) [3, 4, 6, 7].

The plus sign in front of the second term on the right side of equation (6) corresponds to the water flow in the positive direction of the x-axis (in Fig. 1 from the pump to the pressure basin), and the minus sign corresponds to the water movement in the opposite direction.

To integrate the system of equations (2), (3), and (6), all parameters included in them are presented in dimensionless quantities [3, 4, 6, 7]:

$$\bar{z} = \frac{z}{H_{0-a}};\ \bar{\vartheta} = \frac{\vartheta}{\vartheta_0};\ \bar{t} = \frac{t}{T};\ \bar{h}_{mp} = \frac{h_\omega}{H_{0-a}};\ \bar{V}_1 = \frac{V_1}{V_\Gamma};$$

then $d\vartheta = \vartheta_0 d\bar{\vartheta}$, $dt = Td\bar{t}$ and $dV_1 = V_\Gamma d\bar{V}_1$,
where ϑ_0 is steady flow velocity of the fluid in the pressure pipeline.
The oscillation period of the pressure in the damper T can be calculated by taking into account the polytropic process by the formula [3,4]

$$T = \frac{8{,}1V_\Gamma}{\omega\vartheta_0}\sqrt{\sigma} \qquad (7)$$

Where ω is cross-sectional area of the pressure pipeline; σ is characteristic parameter of the damper, which is determined by the formula [3, 4, 6, 7].

$$\sigma = \frac{\omega l \vartheta_0^2}{2gH_{0-a}V_\Gamma} \qquad (8)$$

Taking into account the above equation (2), we can write

$$dV_1 = 8{,}1\bar{\vartheta}\sqrt{\sigma}dt \qquad (9)$$

Accordingly, equation (3) takes the form [3, 4, 6, 7]:

$$\bar{V} = \left(\frac{1}{1+\bar{z}}\right)^{0{,}833} \qquad (10)$$

In equation (3) denoted $\bar{V} = V / V_\Gamma$ and $H=H_{0-a}+z$.
Equation (6), after some mathematical transformations, can be written in the following form

$$d\bar{\vartheta} = \frac{2{,}62}{\sigma}\left(\bar{z} \pm \bar{h}_{mp}\right)d\bar{t} \qquad (11)$$

Head losses during unsteady fluid motion are expressed in terms of losses in a steady state, while it is assumed that $\lambda_{nu}=\lambda$, as proved in [6, 7], where λ is the coefficient of hydraulic resistance in a steady state.

$$\bar{h}_{mp} = \frac{h_{mp0}}{H_{0-a}}\left(\frac{\vartheta}{\vartheta_0}\right)^2 = \bar{h}_{mp0}\bar{\vartheta}^2 \qquad (12)$$

where h_{mp0} and $\bar{h}_{mp0}$ are head losses and dimensionless head losses in steady state.
The pressure spent on hydraulic resistance, known [3, 4, 6, 7], is not completely restored during hydraulic shock. Given this circumstance

$$\bar{h}_{mp} = \eta \bar{h}_{mp0} \bar{\vartheta}^2 = h_n \bar{\vartheta}^2 \qquad (13)$$

where η is coefficient taking into account the restoration of pressure losses (η=0.5÷0.7) [6,7];

$$\bar{h}_n = \eta \bar{h}_{mp0} .$$

Taking into account equality (13), equation (11) takes the form

$$d\bar{\vartheta} = \frac{4{,}05}{\sqrt{\sigma}} \left(\bar{z} \pm \eta \bar{h}_{mp0} \bar{\vartheta}^2 \right) d\bar{t} \qquad (14)$$

To simplify the integration of the system of equations (9), (10), and (14), the notation [3,4,6] is introduced:

$$L = \frac{4{,}05}{\sqrt{\sigma}} \eta \bar{h}_{mp0}; \quad M = \frac{4{,}05}{\sqrt{\sigma}} \bar{z}; \quad N = 8{,}1\sqrt{\sigma} .$$

Then equation (14) takes the form

$$d\bar{\vartheta} = \left(M \pm L\bar{\vartheta}^2 \right) d\bar{t} \qquad (15)$$

Accordingly, equation (9) will be presented in the form

$$d\bar{V}_1 = N\bar{\vartheta} d\bar{t} \qquad (16)$$

First, the first half of the period of the pressure change process is considered, at which, after the pump is turned off, water by inertia continues to flow from the pump to the pressure basin (see Fig. 1). No new portions of water enter the pipeline, so the pressure in it and the damper decreases. Water from the damper partially flows into the pipeline and reduces the pressure drop while the air in the damper expands. In the mathematical analysis of this process in equation (6), the second term on the right side is preceded by a plus sign, and in equation (15), respectively, by a minus sign. Then from equation (15), it follows

$$\int \frac{d\bar{\vartheta}}{ML^{-1} - \bar{\vartheta}^2} = \int L d\bar{t} .$$

Or

$$arth\bar{\vartheta}\sqrt{LM^{-1}} = \left(L\bar{t} + C \right)\sqrt{ML^{-1}} \qquad (17)$$

where C is constant of integration.

Equality (17) was obtained under condition $\bar{\vartheta} < \sqrt{ML^{-1}}$, but it can be proved that the final formula for determining $\bar{\vartheta}$, derived below, is also valid for $\bar{\vartheta} \geq \sqrt{ML^{-1}}$. Equation (17) implies

$$\bar{\vartheta} = \sqrt{ML^{-1}} th\left(L\bar{t} + C \right)\sqrt{ML^{-1}} \qquad (18)$$

Initial conditions: $\bar{t}=0$, $\vartheta=\vartheta_0$, i.e. $\bar{\vartheta}=1$,
Then $C=\sqrt{LM^{-1}}arth\sqrt{LM^{-1}}$.
Where

$$\bar{\vartheta}=\sqrt{ML^{-1}}th\left(L\bar{t}+\sqrt{LM^{-1}}arth\sqrt{LM^{-1}}\right)\sqrt{ML^{-1}} \tag{19}$$

After transformations, formula (19) has the form

$$\bar{\vartheta}=1+\frac{\left(ML^{-1}-1\right)e^{2i\sqrt{LM}}}{\sqrt{ML^{-1}}-1+\left(\sqrt{ML^{-1}}+1\right)e^{2i\sqrt{LM}}}-\frac{ML^{-1}-1}{\sqrt{ML^{-1}}-1\left(\sqrt{ML^{-1}}+1\right)e^{2i\sqrt{LM}}} \tag{20}$$

Expression (20) is substituted into equation (16), which, after integration rewritten as

$$\bar{V}_1=N\bar{t}+N\left(ML^{-1}-1\right)\int\frac{e^{2i\sqrt{LM}}d\bar{t}}{\sqrt{ML^{-1}}-1+\left(\sqrt{ML^{-1}}+1\right)e^{2i\sqrt{LM}}}-N\left(ML^{-1}-1\right)\int\frac{d\bar{t}}{\sqrt{ML^{-1}}-1+\left(\sqrt{ML^{-1}}+1\right)e^{2i\sqrt{LM}}}+C_1= \tag{21}$$
$$=N\bar{t}+\frac{N(M-L)\ln K}{2L\left(M+\sqrt{LM}\right)}-\frac{N(M-L)}{L}\left[\frac{\bar{t}}{\sqrt{ML^{-1}}-1}-\frac{\ln K}{2\left(M-\sqrt{LM}\right)}\right]+C_1,$$

where indicated

$$K=\sqrt{ML^{-1}}-1+\left(\sqrt{ML^{-1}}+1\right)e^{2i\sqrt{LM}} \tag{22}$$

C_1 is constant of integration.
Initial conditions for determining C_1:
for $\bar{t}=0$, $\bar{V}_1=0$ and $K=2\sqrt{ML^{-1}}$, then from (21) it follows

$$C_1=\frac{N(M-L)}{2L\left(M+\sqrt{LM}\right)}\ln 2\sqrt{ML^{-1}}-\frac{N(M-L)}{2L\left(M-\sqrt{LM}\right)}\ln 2\sqrt{ML^{-1}}=-\frac{N}{L}\ln 2\sqrt{ML^{-1}}. \tag{23}$$

Expression (23) is substituted into equation (21), which after transformation, takes the form

$$\bar{V}_1=-N\sqrt{MK^{-1}}\bar{t}+\frac{N}{L}\ln K-\frac{N}{L}\ln 2\sqrt{ML^{-1}} \tag{24}$$

To determine the point in time $\bar{t}$ at which the maximum increase in volume $\bar{V}_1$ occurs, the derivative $d\bar{V}_1/d\bar{t}$ is calculated and equal to zero, i.e.,

$$\bar{V}_1=-N\sqrt{\frac{N}{L}}+\frac{N\left(ML^{-1}+1\right)\cdot 2\sqrt{LM}\,e^{2i\sqrt{LM}}}{L\left[\sqrt{ML^{-1}}-1+\left(\sqrt{ML^{-1}}+1\right)e^{2i\sqrt{LM}}\right]}=0 \tag{25}$$

where

$$\bar{t}=\frac{1}{2\sqrt{LM}}\ln\left(\frac{\sqrt{M}-\sqrt{L}}{\sqrt{M}+\sqrt{L}}\right) \tag{26}$$

Formula (26) is substituted into (24), resulting in

$$\bar{V}_1 = \frac{N}{2L}\ln\left(1 - LM^{-1}\right) \tag{27}$$

Since the value of M is always negative when the pressure drops, the increase in air volume in the damper $\bar{V}_1$ is always positive.
The total air volume in the damper is determined by the formula (10); in this formula $\bar{V} = 1 + \bar{V}_1$, since $V = V_\Gamma + V_1$.
Then formula (10) takes the form

$$1 + \bar{V}_1 = \left(\frac{1}{1+\bar{z}}\right)^{0,833} \tag{28}$$

Or

$$1 + \frac{N}{2L}\ln\left(1 - LM^{-1}\right) = \left(\frac{1}{1+\bar{z}}\right)^{0,833} \tag{29}$$

since $N/2L = \sigma/\eta\bar{h}_{mp}$ and $LM^{-1} = \pi\bar{h}_{mp}/\bar{z}$.
Under these conditions, equation (29) takes the final form

$$1 + \frac{\sigma}{\eta\bar{h}_{mpo0}}\ln\left(1 - \frac{\eta\bar{h}_{mpo0}}{\bar{z}}\right) = \left(\frac{1}{1+\bar{z}}\right)^{0,833} \tag{30}$$

3 Results and Discussion

The joint solution of equations (8), (28), and (30) makes it possible to determine the head drop $z_{\min} = \bar{z}H_{0-a}$ and the minimum absolute head $H_{min}=H_{0\text{-}a}\text{-}z_{min}$ (see Fig. 1), as well as the maximum air volume in the damper $V=V_{max}$. However, this solution is somewhat difficult since the value $\bar{z}$ enters equation (30) in an implicit form.
During the second half of the pressure change period, the liquid flows from the head basin to the pump and compresses the air in the damper (see Fig. 1). In this case, as indicated above, the plus sign is put in equation (15), and after integration, it takes the form

$$\int \frac{d\bar{\vartheta}}{\bar{\vartheta}^2 + ML^{-1}} = L\int d\bar{t}$$

or

$$\sqrt{LM^{-1}}\,arctg\frac{\bar{\vartheta}}{\sqrt{ML^{-1}}} = L\bar{t} + C_2 \tag{31}$$

C_2 is constant of integration.
It was indicated above that at the maximum increment of the air volume in the damper, i.e., at $\vartheta=0$, the time $\bar{t}$ is determined by the formula (26). After substitution into equation (31) $\bar{\vartheta}=0$ and $\bar{t}$, determined from (26), it turns out

$$C_2 = -L\bar{t} = -\frac{L}{2\sqrt{LM}}\ln\left(\frac{\sqrt{M}-\sqrt{L}}{\sqrt{M}+\sqrt{L}}\right) = -0,5\sqrt{LM^{-1}}\ln\varphi \tag{32}$$

where

$$\varphi = \frac{\sqrt{M} - \sqrt{L}}{\sqrt{M} + \sqrt{L}}.$$

Expression (32) is substituted into (31), then

$$\sqrt{LM^{-1}}\, arctg \frac{\bar{\vartheta}}{\sqrt{ML^{-1}}} = L\bar{t} - 0{,}5\sqrt{LM^{-1}} \ln\varphi \tag{33}$$

Where

$$\bar{\vartheta} = \sqrt{ML^{-1}}\, tg\left(\sqrt{LM}\,\bar{t} - 0{,}5\ln\varphi\right) \tag{34}$$

The last equality is substituted into equation (16), which after integration, takes the form

$$\bar{V}_1 = -\frac{N}{L}\ln\cos\left(\sqrt{LM}\,\bar{t} - 0{,}5\ln\varphi\right) + C_3 \tag{35}$$

where C_3 is integration constant;

At $\bar{V}_1$=0, the flow velocity is directed towards the pumping unit, i.e.,

ϑ=-ϑ_0 and $\bar{\vartheta}$=-1, then from equation (33), it turns out

$$\bar{t} = \frac{0{,}5}{\sqrt{LM}}\ln\varphi - \frac{1}{\sqrt{LM}}\, arctg\sqrt{LM^{-1}} \tag{36}$$

To determine C_3, the following are substituted into equation (35):

$\bar{V}_1$=0 and time $\bar{t}$ calculated by the formula (36), then

$$C_3 = \frac{N}{L}\ln\cos\left(arctg\sqrt{LM^{-1}}\right) \tag{37}$$

The last expression is substituted into equation (35), therefore,

$$\bar{V}_1 = -\frac{N}{L}\ln\cos\left(\sqrt{LM}\,\bar{t} - 0{,}5\ln\varphi\right) + \frac{N}{L}\ln\cos\, arctg\sqrt{LM^{-1}} \tag{38}$$

The maximum increment of volume $\bar{V}_1$, and hence the minimum volume of air into the dampers, occurs at time $\bar{t}$, calculated from the expression

$$\bar{V}_1 = -\frac{N\sqrt{LM}\left[-\sin\left(\sqrt{LM}\,\bar{t} - 0{,}5\ln\varphi\right)\right]}{L\cos\left(\sqrt{LM}\,\bar{t} - 0{,}5\ln\varphi\right)} = 0,$$

Where

$$\bar{t} = \frac{\ln\varphi}{2\sqrt{LM}} \tag{39}$$

Under these conditions, from equality (38), after transformations, we obtain

$$\bar{V}_1 = -\frac{N}{L}\ln\sqrt{(L+M)M^{-1}} \tag{40}$$

Since L+M>M and $\ln\sqrt{(L+M)M^{-1}}$ are always positive; therefore, the volume increment of $\overline{V}_1$ is always negative.
Formula (40) is substituted into equation (28), resulting in

$$1-\frac{N}{L}\ln\sqrt{(L+M)M^{-1}}=\left(\frac{1}{1+\bar{z}}\right)^{0,833} \tag{41}$$

or taking into account the accepted notation

$$1-\frac{2\sigma}{\eta\bar{h}_{mp0}}\ln\sqrt{1+\frac{\eta\bar{h}_{mp0}}{\bar{z}_1}}=\left(\frac{1}{1+\bar{z}_1}\right)^{0,833} \tag{42}$$

With a joint solution of the obtained equations (8), (28), and (42), it is possible to determine the increase in head $z_{\max}=\bar{z}_1 H_{0-a}$, the maximum absolute head $H_{max}=H_{0-a}+z_{max}$ (see Fig. 1), as well as the minimum air volume in the damper $V=V_{min}$.
The results of analytical calculations and experiments of the pneumohydraulic damper [3,4] are shown in Table 1. According to Table 1, graphs for comparing the results of experiments and calculations were plotted (Fig. 2).

Table 1. Results of research and calculation of pneumohydraulic damper

S/n	Initial data and results of experiments on the study of the damper						
	ϑ_0, *m/s*	H_{oa}, *m*	H_{ga}, *m*	W_0, m^3	σ	$\bar{h}_{mp0}$	$\overline{Z}^{on}_{\min}/\overline{Z}^{on}_{\max}$
1	1.42	51.5	40.0	0.0142	0.174	0.288	0.3150
							0.3375
2	1.92	59.7		0.0074	0.607	0.492	0.5325
							0.6825
3	1.43	51.2		0.0074	0.336	0.280	0.4650
							0.5750
4	0.78	43.5		0.0074	0.100	0.088	0.3400
							0.3575
5	0.75	43.3		0.0074	0.092	0.082	0.2975
							0.2675
6	1.18	47.7		0.0074	0.229	0.192	0.3700
							0.3450
7	1.51	52.7		0.0074	0.375	0.318	0.4175
							0.4000
8	1.92	59.9		0.0074	0.607	0.498	0.4575
							0.4325
9	1.84	58.5		0.0211	0.196	0.462	0.1950
							0.1550
10	1.48	52.5		0.0211	0.127	0.312	0.1950
							0.1325
11	0.80	44.1		0.0211	0.037	0.102	0.1750
							0.1100
12	0.74	43.5		0.0140	0.048	0.088	0.2225
							0.1575

Continuation of table № 1.

S/n	The results of the calculation of the pneumohydraulic damper			
	According to V.S. Dikarevsky n = 1.0		By author n = 1.2	
	$\bar{Z}_{min}^{calc}/\bar{Z}_{max}^{calc}$	% mistakes	$\bar{Z}_{min}^{calc}/\bar{Z}_{max}^{calc}$	% mistakes
1	0.2919	17.33	0.3286	- 4.32
	0.2728	+ 19.17	0.3197	+ 5.27
2	0.4690	+ 11.92	0.5199	+ 2.37
	0.6339	+ 7.12	0.7436	- 8.95
3	0.4103	+ 11.76	0.4550	+ 2.15
	0.5251	+ 8.68	0.6103	- 6.14
4	0.2914	+ 14.29	0.3225	+ 5.15
	0.3398	+ 4.95	0.3875	- 8.39
5	0.2579	+ 13.31	0.2877	+ 3.29
	0.2494	+ 6.77	0.2880	- 7.55
6	0.3282	+ 11.30	0.3679	+ 0.57
	0.3192	+ 7.48	0.3741	- 8.43
7	0.3613	+ 13.46	0.4065	+ 2.63
	0.3484	+ 12.90	0.4117	- 2.92
8	0.3920	+ 14.32	0.4422	+ 3.34
	0.3756	+ 13.16	0.4469	- 3.33
9	0.1815	+ 6.92	0.2138	- 9.64
	0.1218	+ 21.42	0.1466	+ 5.42
10	0.1743	+ 10.62	0.2036	- 4.41
	0.1180	+ 10.94	0.1412	- 6.57
11	0.1396	+ 20.23	0.1596	+ 8.80
	0.0985	+ 10.45	0.1157	- 5.18
12	0.1768	+ 20.54	0.1996	+ 10.29
	0.1392	+ 11.62	0.1622	- 2.98

An analysis of the data in Table 1 and the graph in Fig. 2 shows that the proposed method for calculating the damper is reliable since the proposed method's calculations give good convergence with the results of experiments.

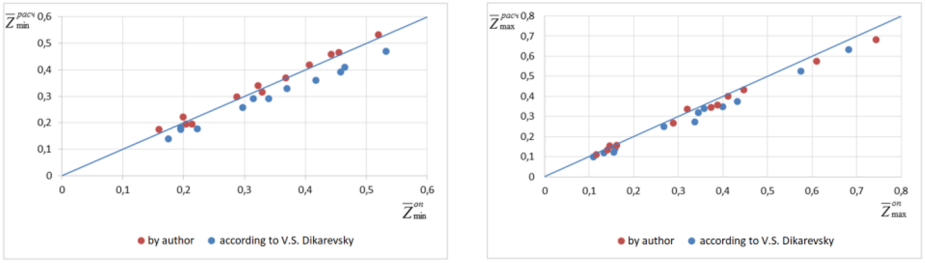

Fig. 2. Comparison of damper calculations with experimental data

The data of Table 1 and the graphs in Fig. 2 also confirm that the polytropic index's value should be equal to n = 1.2 since, in this case, there is some margin of safety in the calculations than with n = 1.0. This provision provides resource saving. To check the reliability of the above dependencies (8), (28), and (42), comparative calculations were performed with the results of experimental data (Table 1). The experiments were carried out in the laboratory of the department "Hydraulics and hydraulic structures" KEEI [3,4].

4 Conclusions

As a result of integrating the equations of unsteady fluid motion, analytical dependences are obtained, which make it possible to determine the parameters of the pneumohydraulic damper with wide variations in the initial parameters.

The value of the polytropic index [3,4] was experimentally determined, and it was recommended to take n = 1.20 when calculating the pneumohydraulic damper.

The results of the experimental studies have proved the reliability of the proposed analytical method for calculating the pneumohydraulic damper installed at the beginning of the pressure pipeline of the pumping station.

References

1. Zhang, B., Wan, W., & Shi, M. Experimental and numerical simulation of water hammer in gravitational pipe flow with continuous air entrainment. Water, 10(7), 928. (2018).
2. Rakhmatulin Kh.A., Mirkhamidova Kh.B. Water hammer in pipes of circular cross section during the movement of multiphase media. - Izv. Academy of Sciences of the Uzbek SSR, ser. tech. Sciences: Mechanics, No. 5, pp. 27-30. (1970).
3. Jonkobilov, U., Rajabov, U., & Jonkobilov, S. Hydraulic shock damper with and without diaphragm. Paper presented at the IOP Conference Series: Earth and Environmental Science, 1112(1) (2022).
4. Jonkobilov, U., Rajabov, U., & Jonkobilov, S. Experimental study of the polytropic coefficient for hydraulic shock from a decrease in pressure. Paper presented at the IOP Conference Series: Earth and Environmental Science, 1112(1) (2022).
5. Evangelisti G. Waterkammer analysis by the Method of characteristics. – L'Energia, Elektrica/Milano, Vol. 86(42), pp.839-858. (1969).
6. Dikarevsky V.S. Conduits. Monograph. Proceedings of RAASN. Construction sciences. Vol. 3 - M.: RAASN, (1997).
7. Dikarevsky V.S., Kapinos O.G. Water supply and sanitation. (2005).
8. Charny I.A. Unsteady motion of a real fluid in pipes. (1975).
9. Fox D.A. Hydraulic analysis of unsteady motion in pipelines (translated from English). Moscow, (1981).
10. Lyamaev B.F., Nebolsin G.P., Nelyubov V.A. Stationary and transient processes in complex hydraulic systems. Computer calculation methods. (1978).
11. J.I.Adachi, E. Detournay, A.P. Peirce, Analysis of the classical pseudo-3D model for hydraulic fracture with equilibrium height growth across stress barriers, Int. J. Rock Mech. Min. Sci. 47, 625–639. (2010)
12. Ghidawi MS, Zhao M, Mclnnis DA, Axworthy DH. A review of water hammer theory and practice. Department of Civil Engineering, The Hong Kong University of Science and Technology, Hong Kong, China. Appl. Mech. Rev. 58:49e76. (2005).
13. Sadafi M, Riasi A, Nourbakhsh SA. Cavitating flow during water hammer using a generalized interface vaporous cavitation model. J Fluids Struct. 34:190–201. (2012).
14. M. Lewandowski, A. Adamkowski, Investigation of hydraulic transients in a pipeline with column separation, J. Hydraul. Eng. ASCE 138 (11) 935–944. (2012).
15. H.A. Kaveh, B.O.N. Faig, K.H. Akbar, Some aspects of physical and numerical modeling of water-hammer in pipelines, Nonlinear Dynam. 60, 677–701. (2010).

16. W. Wan, W. Huang, C. Li, Sensitivity analysis for the resistance on the performance of a pressure vessel for water hammer protection, J. Pressure Vessel Technol. Trans. ASME 136 (1) 011303. (2014).
17. Makisha E.V., Nosorev E.V. Causes and features of the occurrence of hydraulic shock in pressure pipelines of sewage pumping stations. Don Engineering Bulletin, No. 3 (2021).
18. Prigozhaev S.S., Pykhalov A.A., Burmakin N.O. Analysis of the influence of the characteristics of a hydraulic vibration damper on the stress-strain state of a passenger car bogie. Modern technologies. System analysis. Modeling. No. 2 (74). pp. 130–141. (2022).
19. Golovin A.N. Fluid vibration damper with a transversely developed structure. Aviation and rocket and space technology. Proceedings of the Samara Scientific Center of the Russian Academy of Sciences, Vol. 20(4), pp. 76-80. (2018).
20. Ismagilova D.F., Ismagilova R.F., Tselishchev V.A. Mathematical modeling of the hydraulic shock protection system. Bulletin of USATU. Vol. 18 (4(26)). pp. 72–78. (2014).